NIH Public Access
Author Manuscript
Anal Chem. Author manuscript; available in PMC 2014 May 15.

Published in final edited form as:
Anal Chem. 2013 January 2; 85(1): 208–212. doi:10.1021/ac302510g.

Quantitative SERRS Multiplexing of Biocompatible Gold Nanostars for *in vitro* and *ex vivo* detection

Hsiangkuo Yuan, **Yang Liu**, **Andrew M. Fales**, **You Leo Li**, **Jesse Liu**, and **Tuan Vo-Dinh***
Fitzpatrick Institute of Photonics, Departments of Biomedical Engineering and Chemistry, Duke University, Durham, NC 27708, USA

Abstract

Surface-enhanced Raman scattering (SERS)-active plasmonic nanomaterials have become a promising agent for molecular imaging and multiplex detection. To produce strong SERS intensity while retaining the non-aggregated state and biocompatibility needed for bioapplications, we integrated near infrared (NIR) responsive plasmonic gold nanostars with resonant dyes for resonant SERS (SERRS). The SERRS on nanostars was several orders of magnitude greater than signals from SERRS on nanospheres and non-resonant SERS on nanostars. For the first time, we demonstrated quantitative multiplex detection using 4 unique nanostar SERRS probes in both *in vitro* solutions and *ex vivo* tissue samples under NIR excitation. With further optimization, *in vivo* tracking of multiple SERRS probes is possible.

Keywords

Gold nanoparticles; nanostars; surface-enhanced Raman scattering; multiplex detection; in vitro; ex vivo

Introduction

Plasmonic nanomaterial offers great potential for surface-enhanced Raman scattering (SERS) bioapplications. Because SERS detection has less photobleaching and narrower Raman bands (10–20 cm^{-1}) than fluorescence detection (400–800 cm^{-1}),[1] SERS offers superior multiplexing potentials to fluorescence; such bioapplications have been demonstrated on many occasions.[2–7] Although SERS *in vivo* detection has been reported,[8–12] SERS multiplexing *in vivo* remains a challenge mainly due to the low signal-to-noise ratio (SNR) from the weak SERS signal on isolated gold nanoparticles under the near-infrared (NIR) excitation.[13–16] Aggregation or clustering was frequently applied for obtaining higher SERS from “hot-spots” but also resulted in larger particle size distribution and batch-to-batch inconsistency; both of which are unfavorable for practical bioimaging applications. Therefore, our strategy has been focused on (1) creating uniquely-shaped plasmonic nanoparticles with plasmon bands in the NIR range and self-generated “hot-

*Corresponding Author, tuan.vodinh@duke.edu.

ASSOCIATED CONTENT

Supporting Information. Figure S1–5. This material is available free of charge via the Internet at http://pubs.acs.org.

NIH-PA Author Manuscript
NIH-PA Author Manuscript
NIH-PA Author Manuscript

NIH-PA Author Manuscript

NIH-PA Author Manuscript

NIH-PA Author Manuscript

spots" without the need to aggregate nanoparticles, (2) selecting resonant dyes in the NIR range for producing intense surface enhanced resonant Raman scattering (SERRS) signals, and (3) encapsulating each nanoparticle with a protective layer to avoid dye leaching and to reduce aggregation under a physiological environment.

Our group has recently developed plasmon-tunable surfactant-free nanostars (NS) exhibiting strong two-photon photoluminescence and SERS.[17–19] For the last two decades, our laboratory has been involved in the development and application of various SERS plasmonic platforms ranging from nanoparticles, nanopost arrays, nanowires and nanochips.[20–23] A recently developed highly monodisperse gold NS can be a new promising nanomaterial for *in vivo* SERS multiplexing. NS have not only plasmon bands tunable in the NIR tissue optical window,[18] but also multiple sharp branches acting as "hot-spots" for the "lightning rod" effect.[18, 24] Previous studies have shown a superior SERS enhancement factor on NS than on spheres.[19, 25–26] Recent reports also exemplified the potential of biocompatible NS on *in vitro* SERS imaging.[11, 27–29] To further illustrate the feasibility for *in vivo* multiplex detection, the NIR resonant SERS (NIR-SERRS) has been exploited on nanorods or spheres by other groups.[13, 16] SERRS typically has enhancement that is several orders magnitude greater than non-resonant SERS; the maximal SERRS intensity usually coincides with the electronic transition of the dye used.[30–33] Since NS embrace both NIR plasmon and more numerous branches than nanorods, combining NIR resonant dyes on NS may further enhance the SERRS response for practical *in vivo* multiplex detection. To date, although numerous NIR dyes are commercially available, a successful implementation of these dyes for NIR SERRS probe fabrication and multiplex detection has not yet been reported.

In this study, we report a facile synthesis of bovine serum albumin (BSA)-protected NIR-SERRS probes made of plasmonic gold NS. Due to the intrinsically narrow Raman peaks, spectral fitting of the entire fingerprint allows for accurate quantification of each SERRS probe. Quantitative multiplexing of 4 NIR-SERRS probes was achieved in sample solutions (*in vitro*) and then through excised chicken skins (*ex vivo*).

Experimental Methods

Chemicals

Gold (III) chloride trihydrate ($HAuCl_4$), sodium citrate tribasic dihydrate (Na_3Cit), L(+)-ascorbic acid (AA), silver nitrate ($AgNO_3$), hydrochloric acid (HCl), O-[2-(3-mercaptopropionylamino)ethyl]-O'-methylpolyethylene glycol (M_W 5,000; $SHPEG_{5k}$), 4-mercaptobenzoic acid (4-MBA), ethanol (EtOH), methanol (MeOH), sodium dodecyl sulfate (SDS), bovine serum albumin (BSA), phosphate-buffered saline (PBS), NIR dyes (IR-780, IR-792, IR-797, IR-813; Figure S1) were purchased from Sigma-Aldrich (St. Louis, MO). All chemicals were used as received. Millipore Synergy ultrapure water (DI) of resistivity = 18.2 MΩ cm was used in all aqueous solutions. All glassware and stir bars were cleaned with *aqua regia* solution and oven-dried before use. (*Caution: aqua regia is extremely dangerous. Please use it with extra caution.*)

NIH-PA Author Manuscript

NIH-PA Author Manuscript

NIH-PA Author Manuscript

Gold Nanostar NIR-SERRS probe synthesis

Gold nanostars were synthesized using a seed-mediated method modified from our previous report.[18] Briefly, in 10 ml 0.25 mM $HAuCl_4$ solution, 10 μl of 1N HCl and 100 μl of 12 nm citrate gold seeds were added followed by 100 μl of 2 % SDS, 100 μl $AgNO_3$ and 50 μl 100 mM ascorbic acid under stirring (700 rpm). A roughly 0.1 nM of NS was obtained. 10 μl of NIR dyes (1 mM in pure methanol or ethanol) was added under continuous stirring (*ca.* 10^3-10^4 dye molecules per particle). After 1 hour, a final concentration of 0.2 % (w/v) BSA was mixed for another hour. The solution then underwent centrifugation washing (2000–3000 ×g) in PBS 1× and was kept under 4 °C for storage.

Gold nanospheres and silver nanospheres NIR-SERRS probe synthesis

For gold nanospheres, in 10ml 1 mM $HAuCl_4$ solution, 10 μl of 1N HCl and 100 μl of 12 nm citrate gold seeds were added followed by 100 μl of 2% SDS and the addition of 50 μl 100 mM ascorbic acid under stirring (700 rpm). For silver nanospheres, in 10 ml of 100 mM $AgNO_3$ solution, 100 μl of the 12 nm citrate gold seed solution was added followed by 100 μl of 2% SDS and a mixture of 50 μl of 100 mM AA and 10 μl of HCl.[19] Final particle concentrations were approximately 0.15–0.2 nM. A NIR dye (*ca.* 10^3-10^4 dye molecules per particle) was added following the procedure above.

Structural, size, optical, and Raman characterization

Transmission electronic microscopy (Tecnai G^2 Twin, FEI, OR) was used for structural analysis. The particle hydrodynamic size distribution and concentration were determined by nanoparticle tracking analysis (NTA 2.1; build 0342) using NanoSight NS500 (Nanosight Ltd. UK). A UV-VIS spectrophotometer (Shimadzu UV-3600; Shimadzu corporation, Japan) was used to collect the extinction spectrum. A portable Raman spectrometer (Xantus-1, Bayspec, USA) equipped with a 785 nm laser was used for Raman measurement.

SERRS Multiplexing

The freshly prepared NIR-SERRS probes were pre-diluted to obtain similar peak intensities for all probes in the 500–700 cm^{-1} region. The final probe concentrations were within 10~100 pM. The SERRS spectrum from each diluted probe was collected as reference spectra. For *in vitro* study, mixtures of different volume ratios were placed in a glass vial and examined directly through the Raman spectrometer. For *ex vivo* study, layers of chicken skin (*ca.* 1 mm thick/layer) were used to simulate subcutaneous injection. This allows for more control of the tissue thickness. For consistency, only the flat but not the follicle region was used. Chicken skin was kept moist in PBS and laid flat on a coverslip on top of a depression slide containing 70 μl of prediluted NIR-SERRS probes (as probe reference) or NIR-SERRS probes mixture.

The spectral decomposition procedure, which was adapted from Lutz *et al*.,[2] was processed using Matlab (R2012a, MathWorks, MA). The decomposition is based on the assumption that the mixture spectrum comprises of spectra from references and an unknown polynomial. Experimentally, spectra were collected from all references and mixtures. Instead of evaluating a few unique SERRS peaks in a narrow spectral region, whole spectra with

NIH-PA Author Manuscript

NIH-PA Author Manuscript

NIH-PA Author Manuscript

wavenumbers ranging from 200–1500 cm^{-1}, which contains the distinctive Raman signature of each dye, were loaded into Matlab's workspace without any background subtraction. The decomposition process utilizes Matlab functions (lsqr and fmincon) to determine the best fit of the 4 reference spectra to the mixture spectrum. A free-fitting polynomial was introduced to reduce the fitting error.[2] Matlab analysis subsequently generated the minimally constrained coefficients (*i.e.* the fraction) for each reference spectrum and a polynomial background. The final output contains the signal fraction (normalized to 1) of each reference and a polynomial.

Results and discussion

Figure 1A illustrates the schematics of NIR-SERRS probes fabrication. The gold NS were prepared based on our previously reported method but with the addition of 0.02 % sodium dodecyl sulfate (SDS), which formed a bilayer (*ca.* 3~4 nm) on top of the gold surface to stabilize nanoparticles and to ensure their isolated state upon the addition of hydrophobic NIR dyes. Without SDS, a small amount (*e.g.* 10 nM) of NIR dyes destabilize the gold surface causing early aggregation. The presence of SDS not only stabilizes the nanoparticle but also facilitates the adsorption of positively-charged hydrophobic NIR dyes (*e.g.* IR-780, IR-792, IR-797, IR-813) onto the metal nanostar surface, generating strong SERRS intensity upon dye addition (Figure 1B). Furthermore, SDS coated on the anisotropic star-shape, instead of a spherical shape, may entrap more dye molecules onto the NS surface.[26] In contrast, negatively-charged NIR dyes (*e.g.* IR-725, IR-783) showed only fluorescence background (Figure S2). Furthermore, a similar response, but of lower SERRS intensity was also observed on NS coated with poly(sodium 4-styrenesulfonate) (PSS, MW 70,000; data not shown). It is possible that the sulfonate groups of the SDS help to attract positive dyes but keep the negative dyes away from the metal surface. In contrast to PSS, which also has the sulfonate group, the alkyl chains of the SDS may also help to adsorb the hydrophobic portions of the dye.

Combining the SDS-facilitated dye adsorption with NIR responsive dyes and NS, the SERRS responses from these SDS-coated NIR dye-labeled NS were several orders greater than those made of non-resonant dyes or isolated spherical nanoparticles. In a non-aggregated state, SERRS is typically more intense than non-resonant SERS.[30–33] Although NS were previously shown to generate stronger SERS than from spheres under NIR excitation,[19, 25–26] NS labelled of a non-resonant dye (*e.g.* 4-MBA) still has much weaker signal than that from a resonant dye (*e.g.* IR-780; Figure 2A). In addition, NS also outperformed gold and silver spheres under similar experimental conditions (Figure 2B). It is reasonable to believe that the presence of multiple hot spots and NIR plasmon on NS contribute to such a major increment.[19] However, when particles aggregate without the use of SDS, spheres may even generate stronger SERRS than NS (data not shown). Without aggregation, non-resonant SERS on spherical nanoparticles is unlikely to produce sufficient signal for *in vivo* applications. However, SERRS from aggregation is hardly reproducible hence limiting its quantification potential. Therefore, we focused on the synthesis and characterization of non-aggregated SERRS probes in this study.

NIH-PA Author Manuscript

NIH-PA Author Manuscript

NIH-PA Author Manuscript

Nanostars of different plasmon peak positions were investigated for the highest SERRS response. It is generally regarded that the best excitation is slightly blue-shifted with respect to the plasmon maximum.[34] For NIR-SERRS probes of broad plasmon, however, the best excitation may shift towards the opposite direction. It is noteworthy that matching the excitation with the plasmon peak may induce strong surface plasmon resonance but suffer from SERRS signal loss from the background absorption. Such absorption in the Stoke shift region (800–900 nm) for 785-nm excited NIR-SERRS probes has a detrimental effect on the absolute SERRS intensity. By investigating nanostars with plasmon peaks below, at, and above the excitation wavelength, we observed that the less the absorption in the 800–900 nm range the stronger the absolute SERRS intensity (Figure 3).

To achieve biocompatibility and physiological stability, bovine serum albumin (BSA) 0.2 % (w/v) was introduced to the above solutions. Both BSA and PEG have been exploited for enhancing the biocompatibility of nanoparticles for many bioapplications. In our study, BSA was chosen rather than PEG due to its ability to protect the NS from reshaping and aggregating in PBS (Figure S3). Positively-charged BSA may adsorb onto the sulfonate layer or anchor onto the gold metal surface via the cysteine residues on the BSA in order to provide steric protection of NS.[26] BSA also helps to encapsulate the NIR-SERRS probes to prevent leaching of the NIR dyes. The BSA-protected SERRS probes remain SERRS-active for at least two weeks. Encapsulation method for a longer operation lifetime is still under investigation. In addition, it is noteworthy that the BSA-protected probes' isolated state was maintained through multiple washes in PBS; such state was confirmed by the nanoparticle tracking analysis (NTA). In contrast, even though PEGylation has been frequently applied for steric protection, centrifugal washing in PBS led to numerous small clusters, which could be observed through NTA (Figure S3). Such clustering on spherical nanoparticles strongly enhances the SERS signal but suffers from broad size distribution and wide batch-to-batch inconsistency. In short, it is of utmost importance to ensure the biocompatibility and physiological stability of the SERRS probes before introducing to bioapplications.

Quantitative SERRS multiplex detection was first performed using liquid samples in vials (*in vitro)* then through excised chicken skins (*ex vivo*). *In vivo* multiplexing has previously been achieved by simple peak comparison or multivariate spectral fitting.[2, 13, 15–16] Both methods lack the power to decompose broad complex Raman spectra and to identify the signal fraction of each probe from the mixture. Hence, both methods are not suitable for analyzing NIR-SERRS spectra, which typically contain a strong fluorescence background and complex overlapping peaks. To quantitatively decompose complex SERRS spectra without fluorescence subtraction, we applied a spectral decomposition method reported by Lutz *et al.* that was based on the least-square regression using reference spectra and a free-fitting polynomial.[2] Such a method is rapid and easy to implement; it offers satisfactory (< 0.5 % error) fitting results (Figure S4, S5). For *in vitro* multiplexing, different mixing ratios of 4 SERRS probes were placed in glass vials and analyzed through spectral decomposition (Figure S4). The analytical SERRS signal fractions obtained were in good agreement with the predetermined SERRS probe mixing ratios (Figure 4). The spectral decomposition can be achieved in a wide range of concentrations under a short collection time due to high signal-to-noise ratio (SNR) from the NIR-SERRS probes. However, errors and false

NIH-PA Author Manuscript

NIH-PA Author Manuscript

NIH-PA Author Manuscript

positives still existed in the *in vitro* multiplexing, most likely due to the complex overlapping SERRS spectra from NIR dyes of the similar chemical structure superimposed on the low spectral resolution (10 cm^{-1}) from the portable Raman spectrometer used. Upgraded detector and multiple sampling may reduce the error rate. With further refinement, the strong NIR-SERRS together with background subtraction-free spectral decomposition may facilitate the practical application of quantitative SERRS multiplexing.

For *ex vivo* multiplex detection, we examined the SERRS spectra through several layers of chicken skin to mimic the subcutaneous detection in animal. A single layer of skin (*ca.* 1 mm) produces 95% (98% for 2 layers) of signal reduction (Figure 5A), which originates primarily from the tissue scattering/autofluorescence, absorption from NS, and simplistic optical setup. This signal reduction is in agreement with the findings from Mohs *et al*,[35] where the effect of the tissue thickness was fully investigated. We have found that even with the strong SERRS signal, the through-skin intensity from non-aggregated SERRS probes was still not strong enough for proper multiplexing. For measurement through skin, although being excited in the tissue optic window, the tissue autofluorescence added a strong fluorescence background. Furthermore, the tissue scattering greatly reduces the SERRS excitation/collection efficiency through the simplistic portable Raman spectrometer hence generating lower SERRS signal and higher noise; a low SERRS/background ratio together with a low SNR greatly lessens the spectral decomposition quality. To acquire stronger SERRS, data was collected with higher laser power and longer integration. The resulting signal fraction was close to the predetermined ratio but not as good as the *in vitro* ones (Figure 5B, Figure S5). Higher irradiation energy resulted in noticeable heating of the SERRS probes; such phenomenon is favorable for photothermal therapy, but the higher temperature would increase the rate of dye leaching from the metal surface hence more fluorescence background. For future *in vivo* multiplexing experiments, a refined optical setup and multiple sampling with precaution on probe heating will be required. A biocompatible nanoplatform that induces strong absolute SERRS intensity (high SERRS/background ratio) and resists thermal degradation would be ideal. Whether controlled aggregation or isolated NS better suit the *in vivo* applications remains to be studied. With further optimization, *in vivo* SERRS multiplexing can be more achievable.

Conclusion

In this study, we demonstrated the application of plasmonic gold NS to fabricate strong NIR-SERRS probes for *in vitro* and *ex vivo* multiplex detection for the first time. Having both the nanoparticles' plasmons and dyes in the NIR region together with the unique SDS-coated star-shape geometry to entrap more dye produces SERRS signals several orders of magnitude more intense than those with non-resonant dyes or spherical counterparts. Even though a strong fluorescence background is always present in SERRS, quantitative multiplexing can still be achieved with high precision with *in vitro* samples and, to a lesser extent, with *ex vivo* tissue samples. Optimization in probe fabrication, data sampling, and optics design will further improve *in vivo* multiplex SERRS detection.

NIH-PA Author Manuscript

NIH-PA Author Manuscript

NIH-PA Author Manuscript

Supplementary Material

Refer to Web version on PubMed Central for supplementary material.

Acknowledgments

This work was sponsored by the National Institutes of Health (Grants R01 EB006201 and R01 ES014774). AMF is supported by a training grant from the National Institutes of Health (T32 EB001040).

REFERENCES

1. Allgeyer ES, Pongan A, Browne M, Mason MD. Nano Lett. 2009; 9:3816–3819. [PubMed: 19827758]
2. Lutz BR, Dentinger CE, Nguyen LN, Sun L, Zhang J, Allen AN, Chan S, Knudsen BS. ACS Nano. 2008; 2:2306–2314. [PubMed: 19206397]
3. Wang H-N, Vo-Dinh T. Nanotechnology. 2009; 20:065101. [PubMed: 19417369]
4. Matschulat A, Drescher D, Kneipp J. ACS Nano. 2010; 4:3259–3269. [PubMed: 20503969]
5. Kennedy DC, Hoop L-L, Tay KA, Pezacki JP. Nanoscale. 2010; 2:1413–1416. [PubMed: 20820725]
6. Nolan JP, Sebba DS. Methods Cell Biol. 2011; 102:515–532. [PubMed: 21704852]
7. Huang J, Kim KH, Choi N, Chon H, Lee S, Choo J. Langmuir. 2011; 27:10228–10233. [PubMed: 21702512]
8. Qian X-H, Peng X, Ansari DO, Yin-Goen Q, Chen GZ, Shin DM, Yang L, Young AN, Wang MD, Nie S. Nat. Biotechnol. 2008; 26:83–90. [PubMed: 18157119]
9. Stone N, Faulds K, Graham D, Matousek P. Anal. Chem. 2010; 82:3969–3973. [PubMed: 20397683]
10. Yigit MV, Zhu L, Ifediba MA, Zhang Y, Carr K, Moore A, Medarova Z. ACS Nano. 2011; 5:1056–1066. [PubMed: 21194236]
11. Pallaoro A, Braun GB, Moskovits M. Proc. Natl. Acad. Sci. U. S. A. 2011; 108:16559–16564. [PubMed: 21930955]
12. Kircher MF, de la Zerda A, Jokerst JV, Zavaleta CL, Kempen PJ, Mittra E, Pitter K, Huang R, Campos C, Habte F, Sinclair R, Brennan CW, Mellinghoff IK, Holland EC, Gambhir SS. Nat. Med. 2012; 18:829–834. [PubMed: 22504484]
13. von Maltzahn G, Centrone J-H, Park A, Ramanathan R, Sailor MJ, Hatton TA, Bhatia SN. Adv. Mater. (Weinheim, Ger). 2009; 21:3175–3180.
14. Zavaleta CL, Smith BR, Walton I, Doering W, Davis G, Shojaei B, Natan MJ, Gambhir SS. Proc. Natl. Acad. Sci. U. S. A. 2009; 106:13511–13516. [PubMed: 19666578]
15. Wang Y, Seebald JL, Szeto DP, Irudayaraj J. ACS Nano. 2010; 4:4039–4053. [PubMed: 20552995]
16. Maiti KK, Dinish US, Samanta A, Vendrell, K.-S. Soh, S.-J. Park M, Olivo Y-T, Chang M. Nano Today. 2012; 7:85–93.
17. Fales AM, Yuan H, Vo-Dinh T. Langmuir. 2011; 27:12186–12190. (co-first author). [PubMed: 21859159]
18. Yuan H, Khoury CG, Hwang H, Wilson CM, Grant GA, Vo-Dinh T. Nanotechnology. 2012; 23:075102. (co-first author). [PubMed: 22260928]
19. Yuan H, Fales AM, Khoury CG, Liu J, Vo-Dinh T. J Raman Spectrosc. 2012
20. Vo-Dinh T, Hiromoto M, Begun G, Moody R. Anal. Chem. 1984; 56:1667–1670.
21. Vo-Dinh T, Meier M, Wokaun A. Anal. Chim. Acta. 1986; 181:139–148.
22. Vo-Dinh T. TrAC, Trends Anal. Chem. 1998; 17:557–582.
23. Vo-Dinh T, Dhawan A, Norton SJ, Khoury H-N, Wang CG, Misra V, Gerhold MD. J. Phys. Chem. C. 2010; 114:7480–7488.

NIH-PA Author Manuscript

NIH-PA Author Manuscript

NIH-PA Author Manuscript

24. Abalde-Cela S, Aldeanueva-Potel P, Mateo-Mateo C, Rodríguez-Lorenzo L, Alvarez-Puebla RA, Liz-Marzán LM. J. R. Soc. Interface. 2010; 7:S435–S450. [PubMed: 20462878]
25. Li M, Cushing SK, Zhang J, Lankford J, Aguilar ZP, Ma D, Wu N. Nanotechnology. 2012; 23:115501. [PubMed: 22383452]
26. Xie J, Zhang Q, Lee JY, Wang DIC. ACS Nano. 2008; 2:2473–2480. [PubMed: 19206281]
27. Boca S, Rugina D, Pintea A, Barbu-Tudoran L, Astilean S. Nanotechnology. 2011; 22:055702. [PubMed: 21178234]
28. Schütz M, Steinigeweg D, Salehi M, Kömpe K, Schlücker S. Chem. Comm. 2011; 47:4216–4218. [PubMed: 21359379]
29. Rodriguez-Lorenzo L, Krpetic Z, Barbosa S, Alvarez-Puebla RA, Liz-Marzán LM, Prior IA, Brust M. Integr. Biol. 2011; 3:922–926.
30. Cunningham D, Littleford RE, Smith WE, Lundahl PJ, Khan I, McComb D, Graham DW, Laforest N. Faraday Discuss. 2006; 132:135–145. [PubMed: 16833113]
31. McNay G, Eustace D, Smith WE, Faulds K, Graham D. Appl. Spectrosc. 2011; 65:825–837. [PubMed: 21819771]
32. Meyer SA, Ru ECL, Etchegoin PG. J. Phys. Chem. A. 2010; 114:5515–5519. [PubMed: 20377210]
33. Gabudean AM, Focsan M, Astilean S. J. Phys. Chem. C. 2012; 116:12240–12249.
34. Alvarez-Puebla RA. J. Phys. Chem. Lett. 2012; 3:857–866.
35. Mohs AM, Mancini MC, Singhal S, Provenzale JM, Leyland-Jones B, Wang MD, Nie S. Anal. Chem. 2010; 82:9058–9065. [PubMed: 20925393]

NIH-PA Author Manuscript
NIH-PA Author Manuscript
NIH-PA Author Manuscript

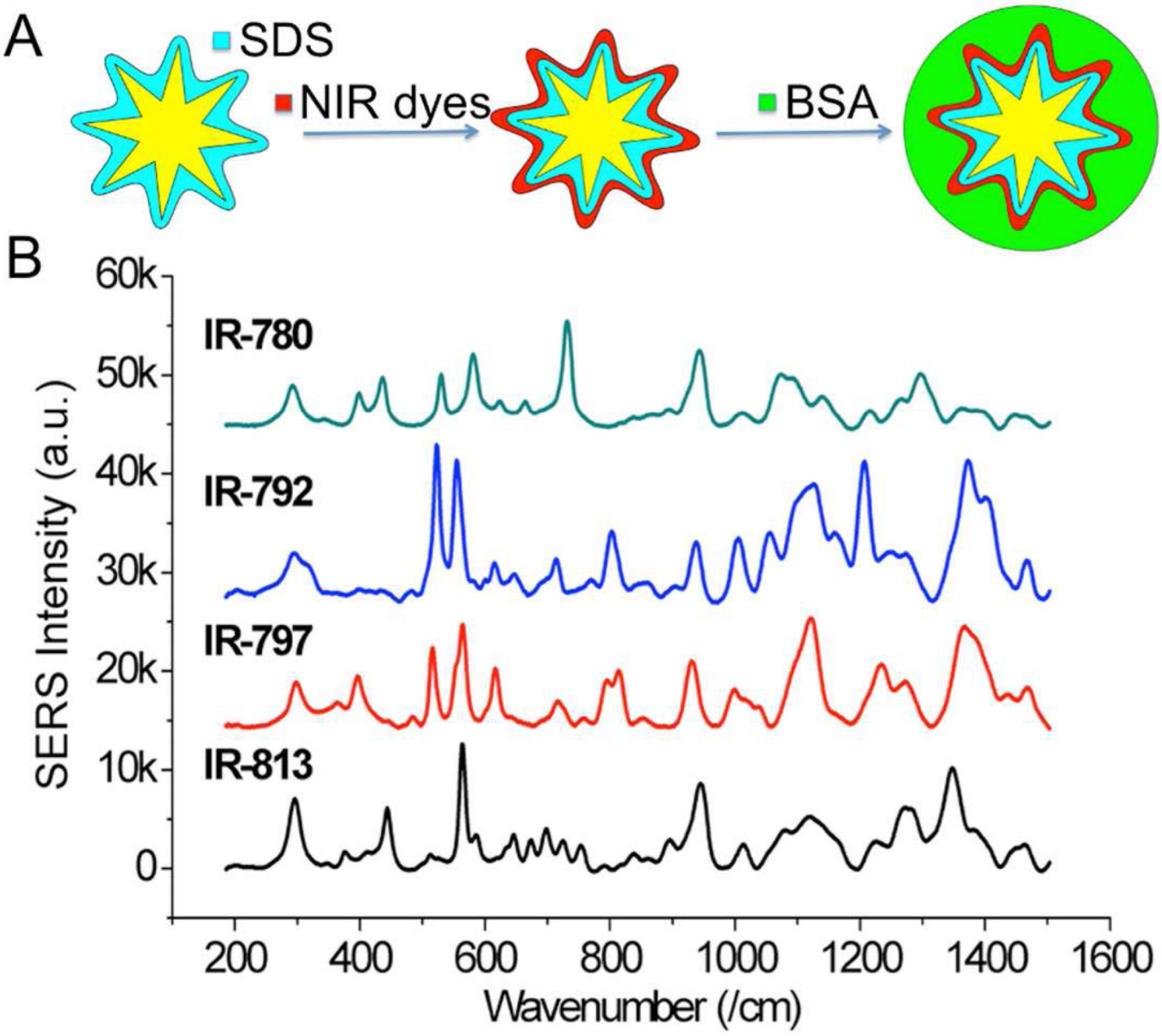

Figure 1.

(A) Schematics of NIR-SERRS probe synthesis. (B) Baseline-subtracted SERS spectra from probes made of 4 different NIR dyes (785 nm excitation, 100 mW, 100 ms, 10 averages).

NIH-PA Author Manuscript
NIH-PA Author Manuscript
NIH-PA Author Manuscript

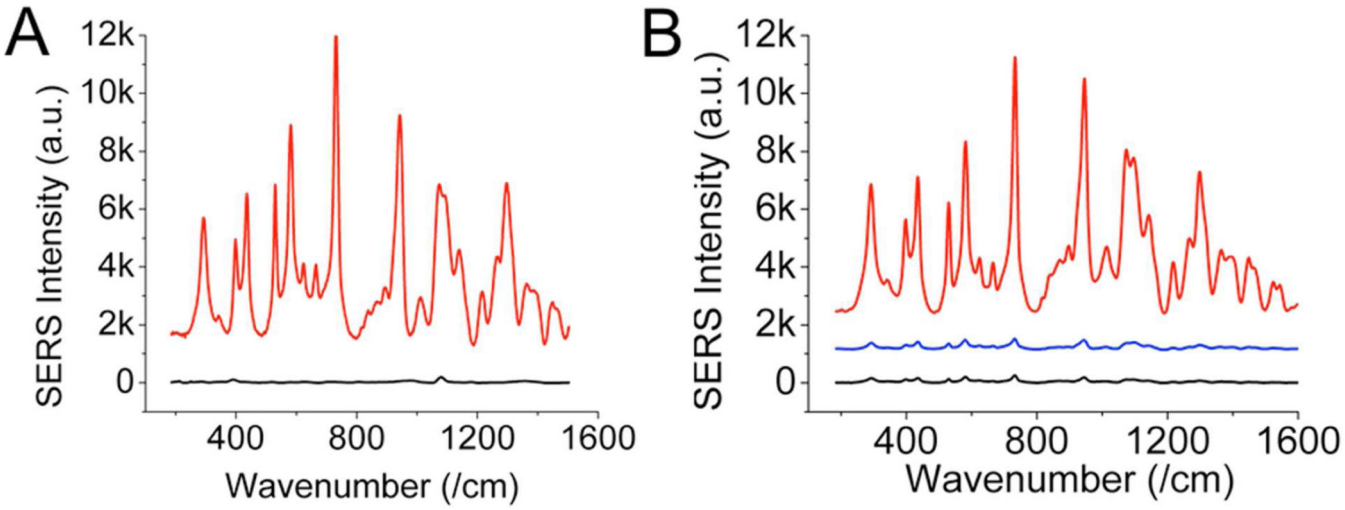

Figure 2.

(A) Baseline-subtracted SERS spectra (offset) from probes made from 1 μM of IR-780 (red) and 4-MBA (black) on NS; SERRS intensity from the former was several orders of magnitude greater than intensity from the latter. (B) Baseline-subtracted SERRS spectra (offset) from 1 μM of IR-780 added onto nanostars (red), gold spheres (blue) and silver spheres (black) of similar sizes. The spectra were collected under 785 nm excitation (100 mW, 100 msec, 10 averages).

NIH-PA Author Manuscript

NIH-PA Author Manuscript

NIH-PA Author Manuscript

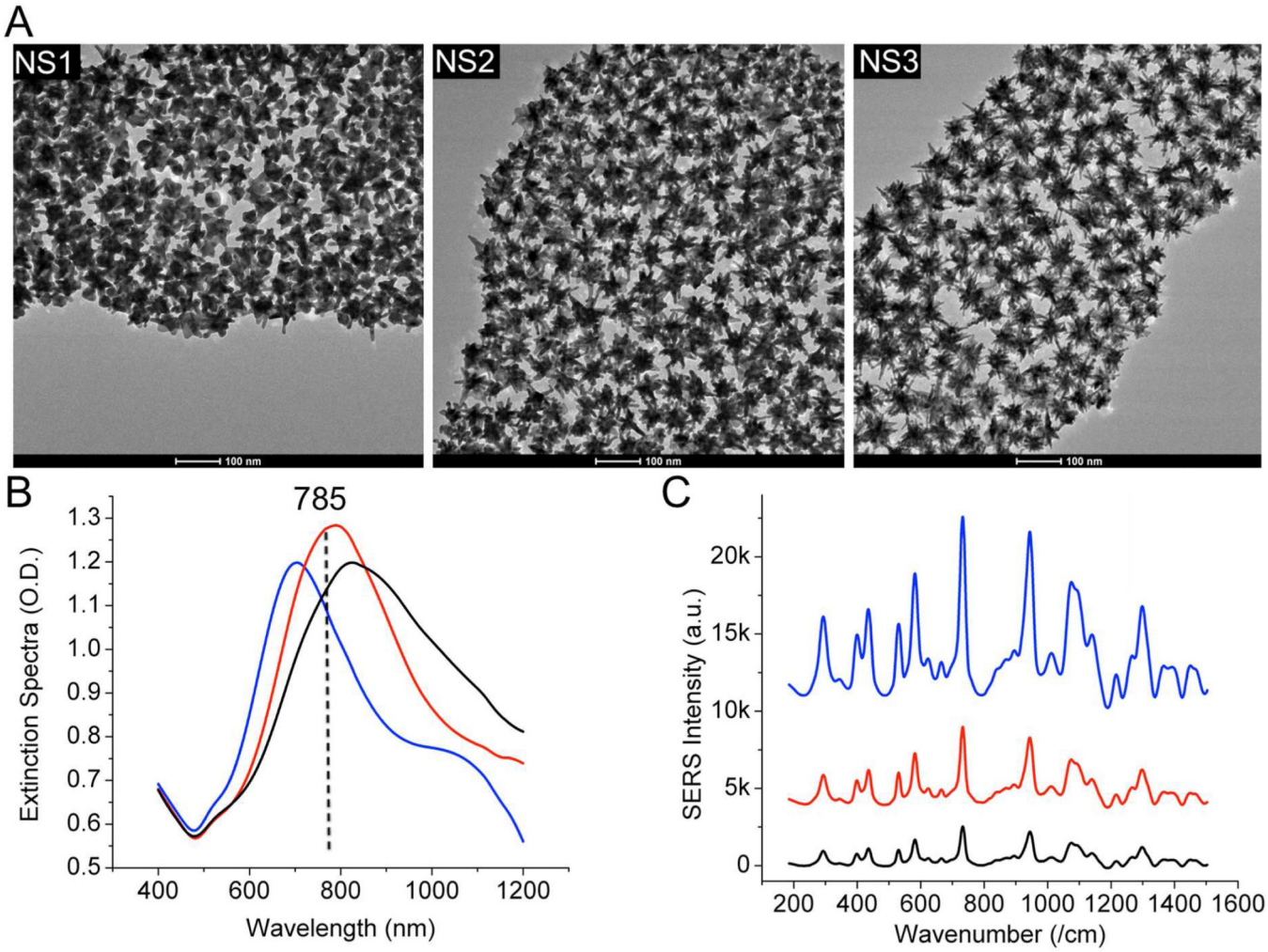

Figure 3.

(A) TEM of 3 types of nanostars (NS1-NS3) investigated. NS3 has the most number of branches. (B, C) Extinction spectra and background-subtracted SERRS spectra (right) of SDS-coated NS1-NS3 labeled with IR-780 1 μM. Even though NS3 has more sharp branches, the SERS intensity was lower than that from NS1, which has less absorption background in the Stoke shift region (800–900 nm). The SERS spectra were collected under 785 nm excitation (100 mW, 100 msec, 10 averages). The dash line is the position of the 785 nm laser.

NIH-PA Author Manuscript

NIH-PA Author Manuscript

NIH-PA Author Manuscript

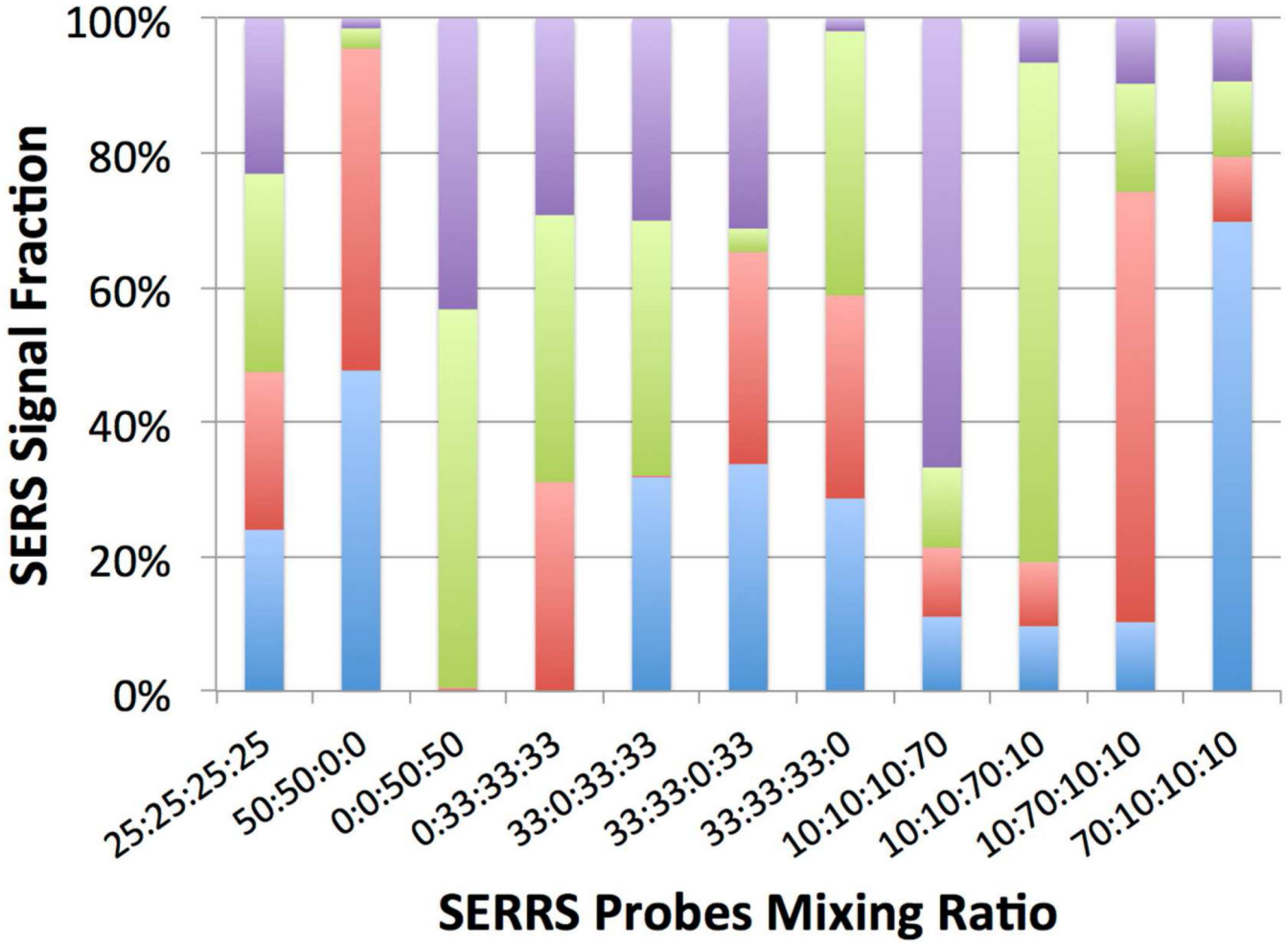

Figure 4.

Quantitative *in vitro* multiplexing of 4 SERRS probes (10–100 pM; blue: IR-780, red: IR-792, green: IR-797, purple: IR-813). Spectral range of 200–1500 wavenumbers was used for analysis. An error (the average difference between measured fractions and the predetermined ratio) of 9.6±3.7 %. Data was collected under 785 nm excitation (200 mW, 500 ms, 10 averages).

NIH-PA Author Manuscript

NIH-PA Author Manuscript

NIH-PA Author Manuscript

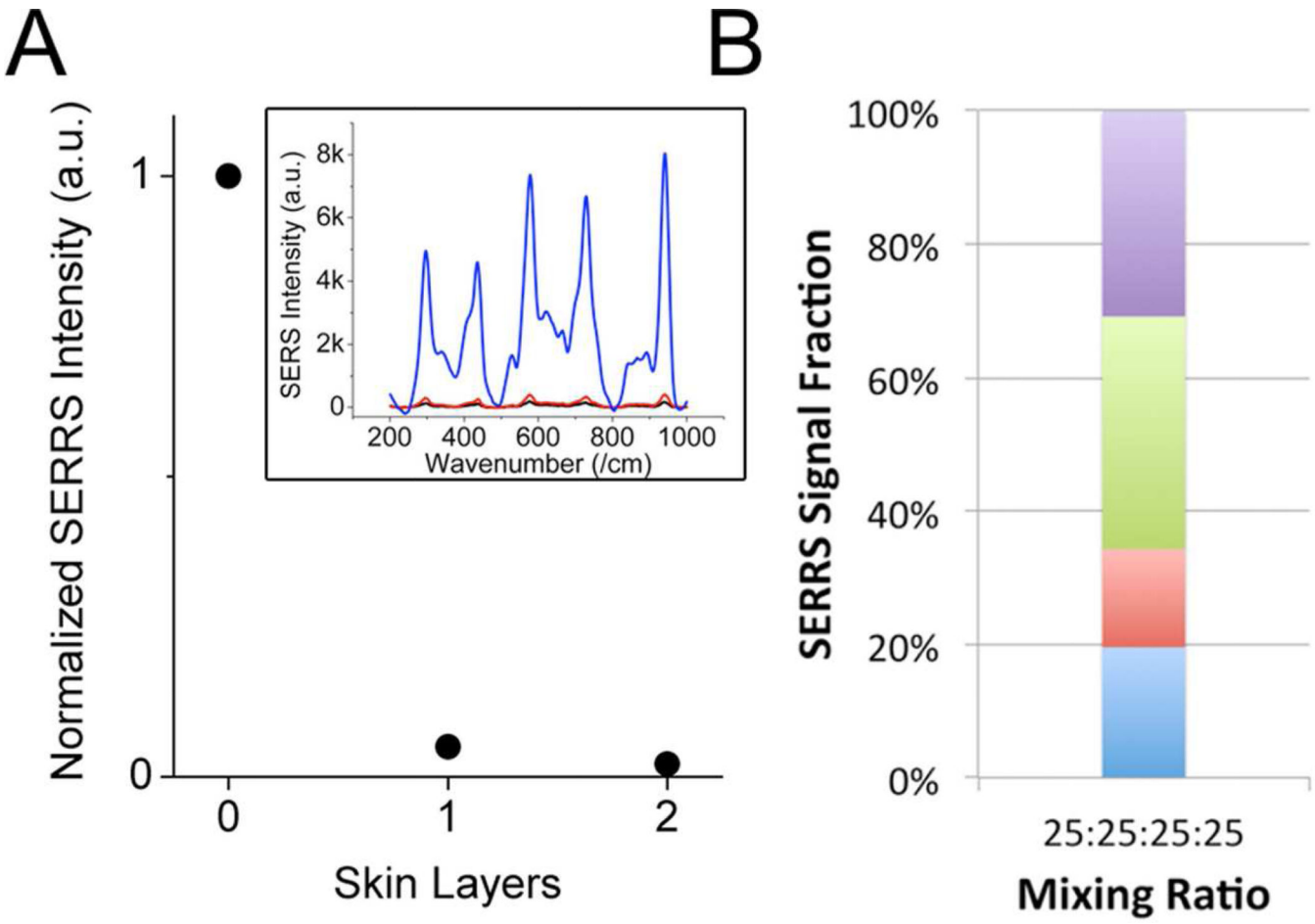

Figure 5.

(A) Normalized SERRS intensity through layers of chicken skin. Error bars are in the black dot. (inset) Background subtracted SERRS spectra through 0 (blue), 1 (red), 2 (black) layers of chicken skin. (B) Quantitative *ex vivo* SERRS multiplexing of 4 SERRS probes (blue: IR-780, red: IR-792, green: IR-797, purple: IR-813). An error of 30.2±3.0 % was observed. Data was collected under 785 nm excitation (400 mW, 10 sec, 1 accumulation).